Cellular Signalling 27 (2015) 777–788

Contents lists available at ScienceDirect

Cellular Signalling

journal homepage: www.elsevier.com/locate/cellsig

T cell tyrosine phosphorylation response to transient redox stress

Christian Secchi [a,b], Marissa Carta [a], Claudia Crescio [a], Alessandra Spano [a], Marcella Arras [c], Giovanni Caocci [d], Francesco Galimi [a,b], Giorgio La Nasa [d], Proto Pippia [a], Francesco Turrini [e], Antonella Pantaleo [a,*]

[a] Department of Biomedical Sciences, University of Sassari, I-07100 Sassari, Italy
[b] Istituto Nazionale Biostrutture e Biosistemi, University of Sassari, I-07100, Sassari, Italy
[c] Haematology, Hospital Binaghi, ASL 8 Cagliari, I-09126, Cagliari, Italy
[d] Haematology, Department of Medical Sciences, University of Cagliari, I-09042 Cagliari, Italy
[e] Department of Genetics, Biology and Biochemistry, University of Turin, I-10126 Turin, Italy

ARTICLE INFO

Article history:
Received 10 November 2014
Received in revised form 9 December 2014
Accepted 24 December 2014
Available online 6 January 2015

Keywords:
Cysteine oxidation
Tyrosine phosphorylation
Inflammation
T cells
Kinases & phosphatases
Syk inhibitors

ABSTRACT

Reactive Oxygen Species (ROS) are crucial to multiple biological processes involved in the pathophysiology of inflammation, and are also involved in redox signaling responses. Although previous reports have described an association between oxidative events and the modulation of innate immunity, a role for redox signaling in T cell mediated adaptive immunity has not been described yet. This work aims at assessing if T cells can sense redox stress through protein sulfhydryl oxidation and respond with tyrosine phosphorylation changes. Our data show that Jurkat T cells respond to –SH group oxidation with specific tyrosine phosphorylation events. The release of T cell cytokines TNF, IFNγ and IL2 as well as the expression of a number of receptors are affected by those changes. Additionally, experiments with spleen tyrosine kinase (Syk) inhibitors showed a major involvement of Syk in these responses. The experiments described herein show a link between cysteine oxidation and tyrosine phosphorylation changes in T cells, as well as a novel mechanism by which Syk inhibitors exert their anti-inflammatory activity through the inhibition of a response initiated by ROS.

1. Introduction

Reactive Oxygen Species (ROS) can be considered not only as a source of oxidative stress but also as triggers or second messengers in intracellular signaling. They can potentially induce and modulate a variety of biological responses including gene expression, cytokine production, differentiation, proliferation and apoptosis [1–4].

Several studies have revealed that ROS may act upon downstream targets within signaling cascades to regulate the activity of enzymes (e.g. phosphatases and kinases) and transcriptional regulators through selective oxidation of the –SH moiety of protein cysteine residues [5,6]. The selective formation of a disulfide bridge through the oxidation of adjacent protein thiols is one of the most likely mechanism of redox sensing due to its reversibility [7,8]. To function as redox sensor a protein is expected to contain –SH groups with a very high reactivity, due to the high concentrations of the intracellular ROS scavenging molecules (GSH, thioredoxin, etc.) [2,8]. Several proteins function as ROS effectors and are reversibly oxidized by ROS. Among the ROS effectors, there are tyrosine phosphatases (PTPs), glycolytic enzymes (GAPDH, enolase), structural proteins (actin, myosin, tropomyosin), regulatory enzymes involved in protein synthesis (elongation factors), folding (heat shock proteins), degradation (ubiquitin, thiolesterases, proteasome components), and antioxidant defense molecules (thioredoxin, peroxiredoxin) [2,9,7,10–13]. Several transcription factors such as NF-KB [14,15], AP-1 [16,17] and c-jun [18,19] are redox-regulated. It has been demonstrated that phosphorylation redox responses are also critical in the activation of several signaling molecules, such as p53, B cell antigen receptor (BCR), JNK/ERK, p38-MAPK, FcγRI, FcεRI, phosphoinositide 3-kinase (PI3K)/AKT, and JAK/STAT [20–25].

Additionally, studies on the redox regulation of erythrocyte membrane stability showed that oxidation of specific cysteine residues, located in the cytoplasmic domain of band 3 protein, induces its tyrosine phosphorylation by Syk [20,26]. This leads to changes in protein–protein interactions that regulate the coupling between cytoskeleton and membrane integral proteins. This phenomenon has been involved in several hemolytic disorders such as β-thalassemia [27], G6PD deficiency [26], sickle-cell anemia [28], and malaria-infected red blood cells (RBCs) [29].

The regulation of the immune system appears to be influenced by its redox state [30,31]. As a matter of fact, chronic inflammation and increased ROS concentrations are involved in different conditions such as Alzheimer's disease [32], Parkinson's disease [33], Crohn's disease [34], systemic lupus erythematosus [35], rheumatoid arthritis [36,37], as well as cardiovascular diseases [38,39].

* Corresponding author. Tel.: +39 079228651; fax: +39 079228615.
E-mail address: apantaleo@uniss.it (A. Pantaleo).

http://dx.doi.org/10.1016/j.cellsig.2014.12.014
0898-6568/

Previous reports have demonstrated the multifaceted effects of ROS on T cells using various experimental models, such as co-culture with monocytes/macrophages or treatments with H_2O_2 [40–43]. Co-culturing T cells with tumor-associated macrophages as a source of ROS and non-cytotoxic concentration of H_2O_2 or diamide resulted in decreased expression of the T cell receptor CD3 zeta chain [43,44]. Moreover, a decrease in CD16 expression was induced in T cells by macrophages isolated from metastatic lymph nodes from patients with malignant melanoma or by LPS-stimulated monocytes [40]. On the other hand, an important work of Baty et al. about Jurkat T cells treated with H_2O_2 indicated the involvement of different redox-sensitive proteins in energy metabolism, protein degradation, structure maintenance and signaling [45]. In 2009 Mougiakakos et al. showed that a subpopulation of T cells, Tregs, differ from other subsets for their resistance to oxidative stress-induced cell death. Suppression assays revealed that high concentration of H_2O_2, highly toxic for helper T cells, did not affect the suppression activity of these cells [46].

Several reports have also demonstrated that ROS mediate leukocytes' recruitment to wounded areas [47–50]. It has been shown that the Lyn kinase is activated by wound-generated H_2O_2, inducing the chemotactic movement of leukocytes [51]. The Cys466 residue in Lyn appears to be the target for oxidants.

Additionally, different reports indicate that protein tyrosine phosphatases (PTPs) may also represent major ROS targets [52,53]. The SH2 domain protein tyrosine phosphatase-2 (SHP-2) is oxidized and inactivated in platelets by ROS leading to the auto-phosphorylation of Syk and additional T cell Tyr kinases [54]. Syk is highly expressed in hematopoietic cells such as B cells, T cells, erythrocytes, mast cells, macrophages and neutrophils [55–57]. Depending on osmotic or oxidative stress, Syk acts in different ways with pro-apoptotic or anti-apoptotic activities. In the latter case, Syk may act in ERK or JUNK pathways (leading to the inhibition of apoptosis) or on the BCR pathway [58]. Syk kinase has been widely studied as a therapeutic target in inflammation [59], neurodegenerative disorders [60], allergy [61] and cancer [62–64]. Besides the studies performed in erythrocytes [26,27,65], the role of cysteine oxidation on Syk activity and functions in T cells are still unknown.

A better understanding of the molecular mechanisms involved in oxidative signaling of T cells may have broad implications for the therapy of different human diseases [66,67]. Due to the complexity of models including cell co-cultures or using H_2O_2, which is rapidly degraded and that can generate ROS reacting in an unpredictable way, we performed experiments with diamide to reversibly oxidize –SH groups.

We used a T cell line (Jurkat T cells) to limit the experimental variability dependent on different blood donors, T cells subsets, and methods used to purify cells. Using low, non-cytotoxic concentrations of diamide, we monitored the phosphorylation response with a proteomic approach and studied the functional involvement of the Lyn and Syk kinases.

2 . Materials and methods

2.1. Cells cultures

Jurkat T cells clone E6.1 were maintained in RPMI 1640 GLUTAMAX (Life Technologies, Carlsbad, CA-USA), supplemented with 10% (v/v) heat-inactivated fetal bovine serum (FBS, Life Technologies, Carlsbad, CA-USA), 20 mM HEPES (Sigma-Aldrich, St.

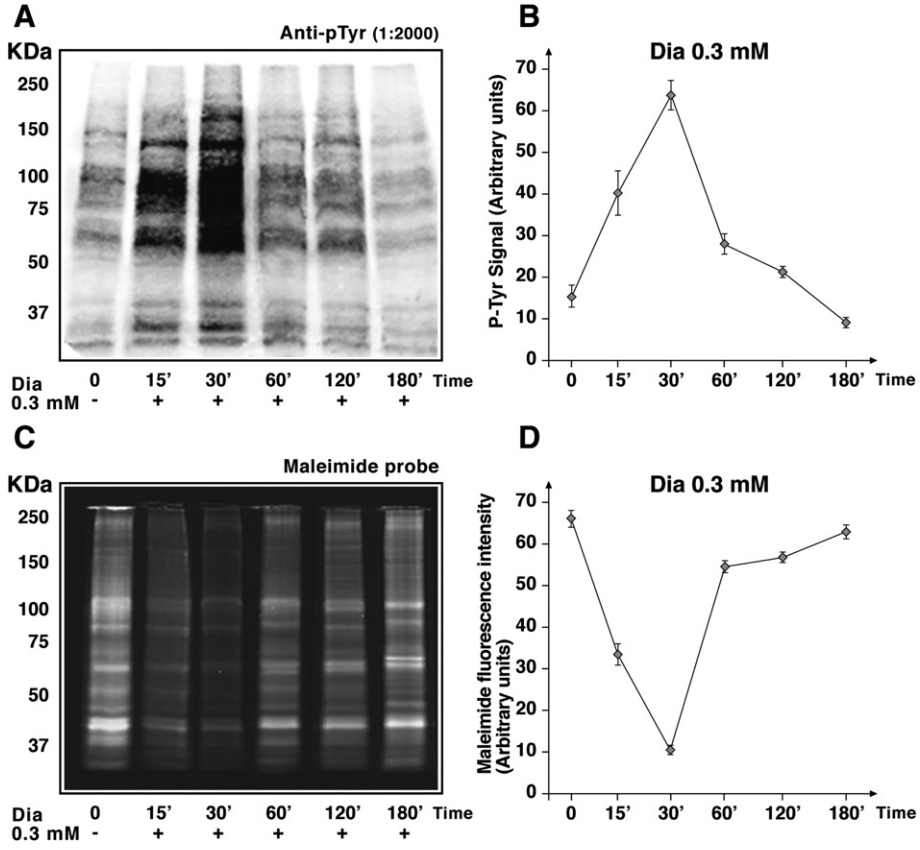

Fig. 1. Time course of the phosphorylation and oxidation of Jurkat T cell total proteins. (A): Anti-phosphotyrosine immunoblot of Jurkat T cell total proteins after 0.3 mM diamide treatment. (B): Quantification of tyrosine phosphorylation levels performed with an IR fluorescence detection scanner (Odyssey, Licor, USA) and expressed as arbitrary units. (C): SDS-PAGE stained with a fluorescent maleimide probe of total Jurkat T cell proteins treated with 0.3 mM diamide. (D). Quantification of oxidation levels performed with an IR fluorescence detection scanner (Odyssey, Licor, USA) and expressed as fluorescence arbitrary units. Values are plotted as mean ± standard deviation of 3 separate experiments.

Table 1
Identification of proteins in Jurkat T cells treated with 0.3 mM diamide by MALDI-ToF.

Number of band	Score	Matched pept.	Name	Mass (Da)	Accession number
1	112	24	Clathrin heavy chain 1	191,493	CLH1_HUMAN
2	71	11	Vinculin	123,799	VINC_HUMAN
3	69	8	Hypoxia up-regulated protein-1	111,335	HYOU1_HIUMAN
4	75	13	N-alpha-acetiltransferasi 15	101,208	NAA15_HUMAN
5	65	9	Nucleolar MIF4G domain containing protein	96,198	NOM1_HUMAN
6	57	11	Endoplasmin	92,411	HSP90B1_HUMAN
7	85	13	Protein kinase C binding protein	91,284	NELL2_HUMAN
8	57	9	Protein FAMM 83 G	90,779	FA83G_HUMAN
9	96	16	Heat shock protein HSP 90-alpha	84,607	HSP90AA1_HUMAN
10	80	14	Heat shock protein HSP 90-alpha	83,212	HSP90B_HUMAN
11	72	8	Prospero homeobox protein	83,151	PROX1_HUMAN
12	79	8	Non-canonical poly (A) RNA polymerase PAPD/	82,309	PAPD/_HUMAN
13	68	16	Protein kinase C theta	81,811	KPCT_HUMAN
14	73	11	Stress-70 protein, mitochondrial	73,635	GRP75_HUMAN
15	79	9	78 kDa glucose-regulated protein	72,288	GRP78_HUMAN
16	56	9	Tyrosine-protein kinase SYK	72,066	KSYK_HUMAN
17	52	11	Heat shock cognate 71 kDa	70,854	HSP7C_HUMAN
18	56	9	WD repeat-containing protein 1	66,152	WDR1_HUMAN
19	95	12	60 kDa heat shock protein, mitochondrial	61,016	CH60_HUMAN
20	68	8	Protein disulfide-isomerase A3	56,747	PDIA3_HUMAN
21	139	14	Tubulin beta chain	49,639	TBB5_HUMAN
22	80	8	Alpha-enolase	47,139	ENOA_HUMAN
23	75	7	Actin, cytoplasmic 1	41,710	ACTB_HUMAN
24	80	7	Fructose-bisphosphate aldolase A	39,395	ALDOA_HUMAN
25	87	9	Glyceraldehyde-3-phosphate dehydrogenase	36,030	G3P_HUMAN

Louis, MO-USA), 100 units/ml penicillin and 100 μg/ml streptomycin (Life Technologies, Carlsbad, CA-USA) at 37 °C in a humidified atmosphere 5% CO_2. The cells were subcultured every 3 days at density of 6×10^5/ml with fresh medium in a 75 cm^2 tissue culture flask (Corning, NY-USA).

2.2. Syk and Lyn inhibitors

Cells were pre-incubated with 5 μM Syk inhibitors II (Calbiochem, San Diego, CA-USA) or 10 μM Lyn Inhibitor (PP2, Calbiochem, San Diego, CA-USA) for 1 h at 37 °C before oxidant treatments. The cells were washed with phosphate buffer saline (PBS) prior to the oxidant treatment.

2.3. Oxidant agent

Transient oxidative stress was induced treating Jurkat T cells with diamide in RPMI 1640, reported to be a specific thiol oxidizing agent [43]. Diamide (Sigma-Aldrich, St. Louis, MO-USA) was firstly tested in dose response experiments and 0.3 mM concentration was chosen for our experiments. Cells were incubated at 37 °C for different times to evaluate the phosphorylation dose response and then washed four times with PBS (150 ×*g*, 10 min). Viability of the cells was examined by Trypan blue dye exclusion test (Sigma-Aldrich, St. Louis, MO-USA) and apoptotic index was assessed by Annexin V assay (Life Technologies, Carlsbad, CA-USA).

2.4. MTT reduction test

To determine reductive activity, $1{,}5 \times 10^5$ cells were pre-incubated with 0.3 mM diamide in RPMI 1640 (90 μl) at different time points in each well of a 96-well plate (Corning, NY-USA). Then, the cells were incubated for 4 h with 10 μl RPMI 1640 medium containing 5 mg/ml Thiazolyl blue tetrazolium bromide (MTT, Sigma-Aldrich, St. Louis, MO-USA). Later, the medium was removed and the converted dye was solubilized with 0.3 ml of a MTT solvent solution constituted by 4 mM HCl, 0.1% Nondet P-40 (NP40) all in isopropanol (Sigma-Aldrich, St. Louis, MO-USA). Absorbance was measured at 570 nm using a microplate reader (Biorad, Hercules, CA-USA) and the reduction activity was expressed as percentage of the corresponding control.

2.5. Electrophoresis and immunoblotting

Total protein content was quantified using DC Protein Assay (Biorad, Hercules, CA-USA) and was solubilized in Laemmli Buffer under reducing conditions (2% beta-mercaptoethanol) in a volume ratio of 1:1. SDS-Page analysis was conducted by heating the samples for 5 min at 100 °C and loading 10 μg total proteins on the 8% gel for protein staining by blue colloidal Coomassie (Sigma-Aldrich, St. Louis, MO-USA). For western blotting analysis, 30 μg of proteins were loaded on each lane and transferred to nitrocellulose membranes. Membranes were blocked in PBS/T (8,5 mM Na_2HPO_4, 1,47 mM KH_2PO_4, 2,68 mM KCl, 137 mM NaCl, 0.1% Tween20) (Sigma-Aldrich, St. Louis, MO-USA). Separated proteins were probed with anti-Syk (Cell signaling, Danvers, MA-USA), anti-pSyk

Table 2
Phosphopeptides of Jurkat T cells treated with 0.3 mM diamide identified by MS/MS spectrometry.

Accession number	Protein name homo sapiens	Identified peptides	Tyrosine number
P06239	Tyrosine-protein kinase Lck	NLDNGGF**Y**ISPR	Y181
Q06124	Tyrosine-protein phosphatase non-receptor type 11 isoform 1/2	IQNTGD**Y**YDLYGGEK	Y62
Q00526	Cyclin-dependent kinase 3	IGEGT**Y**GVVYK	Y15
P06239	Lymphocyte-specific protein tyrosine kinase precursor	SVLEDFFTATEGQ**Y**QPQP	Y505
Q9NTI5	PDS5, regulator of cohesion maintenance, homolog B	HHKSKKGPPRQAK**Y**AIHCIHAIFSSK	Y728
P27695	APEX nuclease	HLYPNTPYAYTFWT**Y**MMNAR	Y269

(Cell signaling, Danvers, MA-USA), anti-phosphotyrosine and/or anti-phosphoserine antibodies (Santa Cruz, Santa Cruz, CA-USA), all diluted 1:2000. Secondary mouse and rabbit antibodies conjugated to infrared fluorescent dyes excitable at 800 nm (IRDye 800CW, Licor, USA) were used (1:25,000) to visualize the desired antigens using an 800 nm laser scanner (Odyssey, Licor, USA). Quantitative analysis of proteins on the membranes was performed by Odyssey software (Licor, USA).

2.6. Maleimide probe

A sulfhydryl-reactive dye (DyLight 800 Maleimide, Thermoscientific, Waltham, MA-USA) was used to study the effects of 0.3 mM diamide treatment. A 30 μl volume of treated and untreated cell pellets was suspended in 30 μl of PBS and incubated with 0.25 mg/ml Maleimide 800 Dye for 1 h at room temperature in complete darkness. The reaction was stopped by washing in PBS-BSA followed by two washes in PBS. The cells were then solubilized for SDS-PAGE. Images were acquired using Odyssey scanner (Licor, USA). Quantitative analysis of the probe bound to the –SH groups of proteins was performed by Odyssey software (Licor, USA).

2.7. Maldi-ToF analysis

Coomassie stained bands were excided from gels and proteins were digested with trypsin. Each piece of gel was de-stained by several washes in 5 mM NH_4HCO_3/acetonitrile (50/50 v/v) and successively dried with pure acetonitrile. The gel slices were rehydrated for 45 min at 4 °C in 20 μl of a 5 mM NH_4HCO_3 digestion buffer containing 10 ng/μl of trypsin (Sigma-Aldrich, St. Louis, MO-USA). The excess of protease solution was removed and the volume adjusted with 5 mM NH_4HCO_3 to cover the gel slices. Digestion was allowed to proceed overnight at 37 °C.

Samples were loaded onto MALDI target using 1 μl of the tryptic digests mixed 1:1 with a solution of alpha-Cyano-4-hydroxycinnamic acid (10 mg/ml in 0.1% acetonitrile/trifluoroacetic acid, 40/60), (Sigma-Aldrich, St. Louis, MO-USA). MS analysis of peptides was performed by a MALDI-TOF Micro MX (Micromass, Manchester, UK) working in reflectron modality according to the tuning procedures suggested by the manufacturer. Peak lists were generated with Proteinlynx Data Preparation using the following parameters: external calibration with lock mass using mass 24,651,989 Da of ACTH fragment 18–39 (Sigma-Aldrich, St. Louis, MO-SA) background subtract with adaptive mode, performing deisotoping with 3% threshold.

For peptide mass fingerprinting (PMF) analysis, the MS spectra were converted into pkl files using Mass Lynx 4.0. Peak lists containing the most intense peaks of the spectrum were sent to MASCOT PMF search (http://www.matrixscience.com) using the Swiss-Prot database. Search settings allowed one missed cleavage with the trypsin enzyme selected, for 1-DE analysis and oxidation of methionine as potential variable modification and a peptide tolerance of 50 ppm. Only protein identifications with significant Mascot scores ($p < 0.05$) were taken in consideration.

2.7.1. Sample preparation and protein digestion protocol for Triple Q-ToF analysis

After lysis of treated Jurkat T cells using a 20% SDS, 1 M DTT, 5 μl benzonase (250 units/μl) and 8 M Urea (Sigma-Aldrich, St. Louis, MO-USA), samples were placed on a Ultra Centrifugal Filter Unit with PLTK Ultracel-30 Regenerated Cellulose Membrane (Billerica, MA-USA) in order to remove the detergent and concentrate proteins. After different washing steps the proteins were ready for trypsin digestion. For our experiments, after incubation with SDS, samples were treated following the protocol by FASP Protein Digestion Kit (Expedeon, San Diego, CA-USA).

2.7.2. Immunoprecipitation

After the tryptic digestion, immunoprecipitation of the tyrosine phosphopeptides was performed. The anti-phosphotyrosine antibody beads (Santa Cruz, Santa Cruz, CA-USA) were activated with an immunoprecipitation buffer (50 mM MOPS pH 7.2,10 mM Sodium Phosphate and 50 mM Sodium Chloride). The samples were incubated with the beads at 4 °C o/n. After this step the beads were washed and the antibodies were freed with 2% TFA and incubated at 55 °C.

Before and after immunoprecipitation C18 Tips (Thermo Scientific Pierce, Waltham, MA-USA) were employed to desalt and concentrate samples. They enabled an efficient purification of peptides and small proteins before mass spectrometry. Finally the pooled samples were dried in cool speed-vac until the volume of 10 μl and added μl 5% FA when ready for MS analysis.

2.7.3. Mass spectrometry and software analysis

Trypsin-digested peptides of Jurkat samples were analyzed for 90 min by HPLC coupled with LC-MS/MS using nano-spray ionization. The nano-spray ionization experiments were performed using a Triple-Tof 5600 hybrid mass spectrometer (AB SCIEX, Framingham, MA-USA) interfaced with an Agilent 1200 capillary nano-scale reversed-phase HPLC system (Agilent Technologies, Santa Clara, CA-USA). All collected data were analyzed using MASCOT (Matrix Sciences), Peak View and Protein Pilot 4.0 (AB SCIEX, Framingham, MA-USA) for peptide identifications.

2.8. Microscopy

Jurkat T cells incubated with diamide and/or Syk inhibitors were pelleted and washed twice in PBS. Then they were fixed for 60 min in 4% PFA. Cells were washed two times and permeabilized in PBS

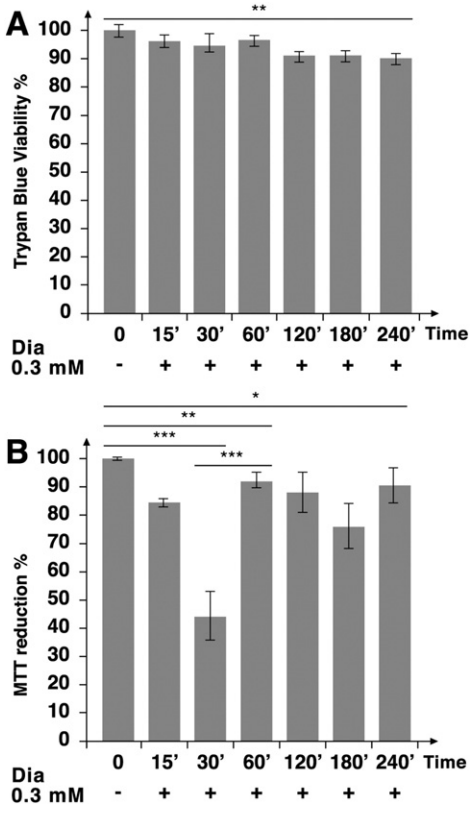

Fig. 2. Trypan blue viability assay and MTT reduction test of Jurkat T cells. (A): Trypan blue assay of Jurkat T cells at different time points (from 15 min to 240 min) of 0.3 mM diamide oxidation. Viability is expressed as percent of total cell number (%). P value of the viability time points was found to be statistically significant by One-way ANOVA Test (**$p < 0.01$). (B): MTT reduction test of Jurkat T cells treated with 0.3 mM diamide. Reduction activity is expressed as percent of untreated cells. Values are plotted as mean ± standard deviation of 3 separate experiments. Medians and P values which were found to be statistically significant by the t-student test are shown (*$p < 0.05$, **$p < 0.01$, ***$p < 0.001$).

containing 0.2% Triton X-100 (Sigma-Aldrich, St. Louis, MO-USA) for 10 min. After the incubation, all non-specific bindings were blocked by an incubation for 60 min at 37 °C with 5% goat serum/PBS. Permeabilized Jurkat T cells were stained by using 1:100 anti-phosphotyrosine antibodies (Santa Cruz Biotechnology, Santa Cruz, CA-USA) and 1:250 mouse FITC-conjugated secondary antibody (Sigma-Aldrich, St. Louis, MO-USA) in PBS/1% goat serum. 1 μg/ml DAPI (Sigma-Aldrich, St. Louis, MO-USA) was added for 1 min. After labeling, resuspended samples were allowed to attach to cover slips coated with polylysine. The samples were observed with a Olympus BX 51 microscope, UplanFL 60X/1.25 Oil Iris Lens, 479–490 excitation filter and 505 dichroic filter, 510–550 emission filter. The images were acquired in the NL with an Optronics-Magnafire camera. The merge and quantification of fluorescence levels were performed using Image J software (ver 1.44p).

2.9. Cytokine release quantification

After the treatment with 0.3 mM diamide and Syk inhibitors supernatant of Jurkat T cell and primary T cells (1.5×10^6 cells for each condition) were collected. The concentrations of soluble cytokines (IL-2, IFNγ, TNFα) in culture supernatants were measured with CBA Flex Set (BD Biosciences, Mountain View, CA, USA). It was used as powerful and accurate analysis to quantify multiple cytokines from the same sample simultaneously. The analyses were performed with the FACS CANTO (BD Biosciences, Mountain View, CA, USA).

2.10. Membrane receptor analysis

T cell functional studies were made by measuring markers expressed on the cell surface of the treated cells. The different expression of several surface receptors like CD25 (IL-2 receptor), CD62L (L-Selectine), HLA-DR, CD45RA + and CD45RO + were studied with specific antibodies for each marker and were purchased from BD Biosciences (Mountain View, CA, USA). They were analyzed with flow cytometry FACS CANTO (BD Biosciences, Mountain View, CA-USA). Experimental data analysis was performed with BD FACS DIVA™ (BD Biosciences, Mountain View, CA-USA).

2.11. Statistical analysis

Data were analyzed by *t*-test performed using Microsoft Excel. All the results were expressed as means +/− SD. $p < 0.05$ was considered statistically significant.

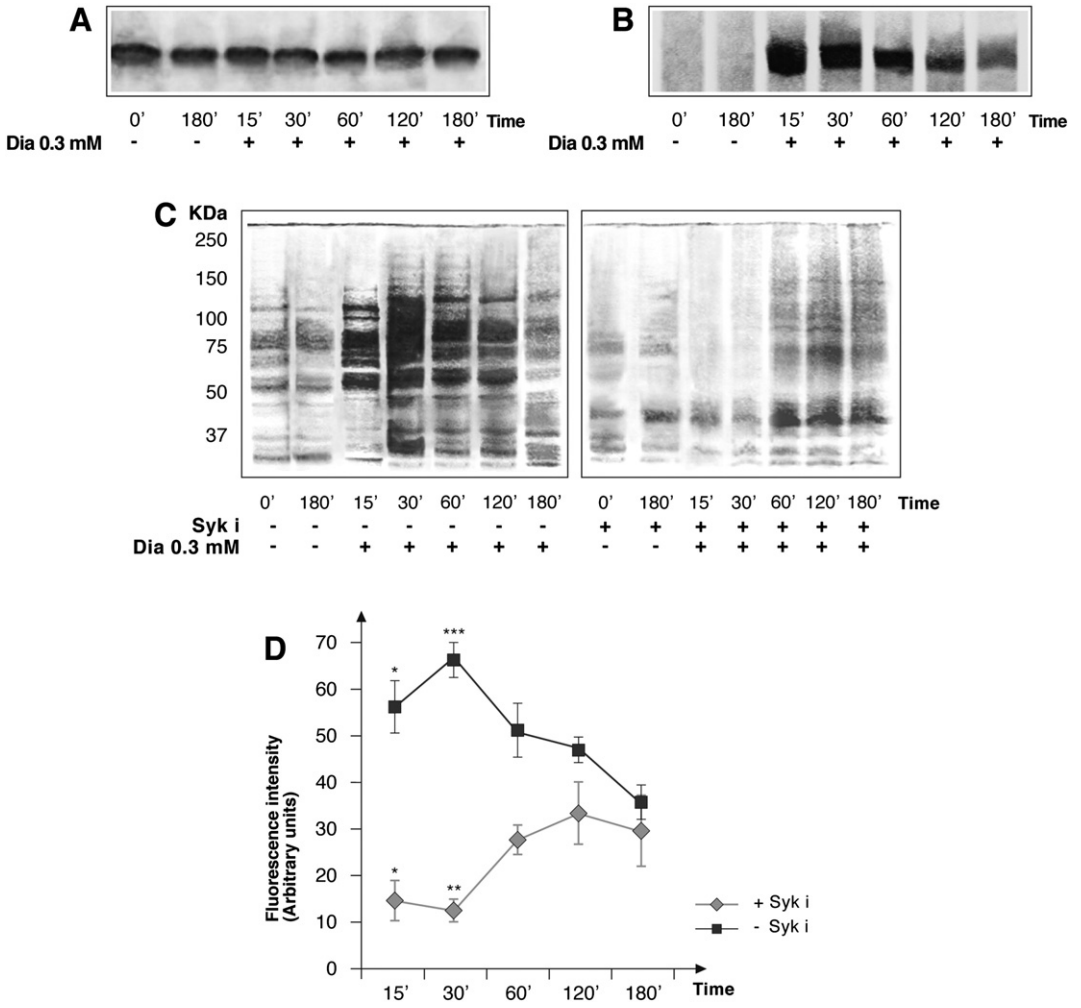

Fig. 3. Role of Syk and activity of Syk inhibitors in the Jurkat T cells under oxidative condition. (A): Immunoblot of Jurkat cell Syk expression time course in oxidative condition; (B): immunoblot of Jurkat cell Syk phosphorylation time course in oxidative condition; (C): Immunoblot of Jurkat T cells treated with 0.3 mM diamide, in the absence or presence of Syk inhibitors 5 μM (Syk i), at different incubation times (0–180 min). (D): Quantification of tyrosine phosphorylation levels was performed by IR fluorescence detection (Odyssey, Licor, USA) of anti-phosphotyrosine western blots and expressed as fluorescence arbitrary units. Values are plotted as mean ± standard deviation of 3 separate experiments. *($p < 0.05$), **($p < 0.01$) and ***($p < 0.001$) indicate the incubation time that determines a statistically significant change by t-student test in comparison to the control sample.

3 . Results

3.1. SH group oxidation elicits a tyrosine phosphorylation response in Jurkat T cell proteins

Diamide is a specific –SH group oxidant that, forming intermediate thiyl radicals, mainly generates reversible disulfide bonds. Its concentration was chosen to observe those changes avoiding cell toxicity (see next paragraph). Jurkat T cells were treated with 0.3 mM diamide. Protein –SH group oxidation and tyrosine phosphorylation changes at different incubation times (15, 30, 60, 120 and 180 min) were measured and both peaked after 30′ incubation (Fig. 1). Of note, those changes are very similar to the response observed in erythrocytes, which display the lowest GSH levels after 30 min and restore basal GSH levels within 60 min [25]. No apparent changes in protein serine phosphorylation have been observed under the same conditions (data not shown).

3.2. Proteomic analysis of tyrosine phosphorylation response in Jurkat T cell proteins

To identify the protein tyrosine phosphorylation sites involved the oxidative and phosphorylation changes initiated by diamide we used different proteomic approaches.

We initially used MALDI-ToF to identify the protein bands showing oxidative and/or phosphorylation changes (Fig. 1). This analysis showed a great complexity of the cellular response activated by oxidation: kinases, structural proteins, and heat shock proteins (HSPs) seemed to be the most intensely affected (Fig. 9 in supplementary data and Table 1), but the analytical limits of this proteomic approach (low specificity due to the difficulty in co-identifying protein bands stained by western blot and Coomassie) persuaded us to carry out a more specific investigation.

In order to gain additional information we designed experiments based on MS/MS identification of immunoprecipitated Tyr phosphopeptides. Phosphorylation analysis was performed in order to detect the unique phosphoTyr-sites of proteins. This phosphorylation-targeted tandem mass spectrometry strategy was focused on scanning the ionized peptides through different quadrupoles: the ions are fragmented through low-energy collisions and then scanned with a fixed offset to the modification and the charge state of the precursor peptide. It permitted to identify 36 proteins and 46 phosphopeptides in untreated and treated samples. Table 2 shows the distinctive Tyr phosphopeptides identified by MS/MS of proteins that we found in treated samples. Our analysis provided preliminary evidences on several plausible effectors such as Lck, AP endonucleases, and Cdk3. Despite these promising results, proteomic data did not provide sufficient information to support a prediction of the cellular effects of protein phosphorylation changes induced by a transient –SH group oxidation. We therefore decided to perform further analysis to obtain a better functional description of the cellular responses (see following sections).

3.3. Cell viability and MTT reduction following diamide treatment

In order to confirm the viability of Jurkat T cells after diamide treatment, Trypan blue exclusion test was performed (Fig. 2A) showing that viability was not apparently affected. Fig. 2B shows the capability of cells to reduce Thiazolyl Blue Tetrazolium Bromide (MTT) at different incubation times with diamide. This test is in agreement with the temporal changes of protein –SH groups, showing a transient decrease of the cellular reductive activity after 30 min and a subsequent recovery within 60 min.

At higher concentration of diamide increasing loss of viability was observed. Moreover apoptosis index was analyzed by Annexin V assay showing that diamide treatment did not induce apoptotic phenomena (data not shown).

3.4. Spleen tyrosine kinase (Syk) is involved in tyrosine phosphorylation changes induced by –SH group oxidation

Next we investigated the role of Syk in the tyrosine phosphorylation cascade triggered by diamide. Fig. 3A shows that Syk appears to be

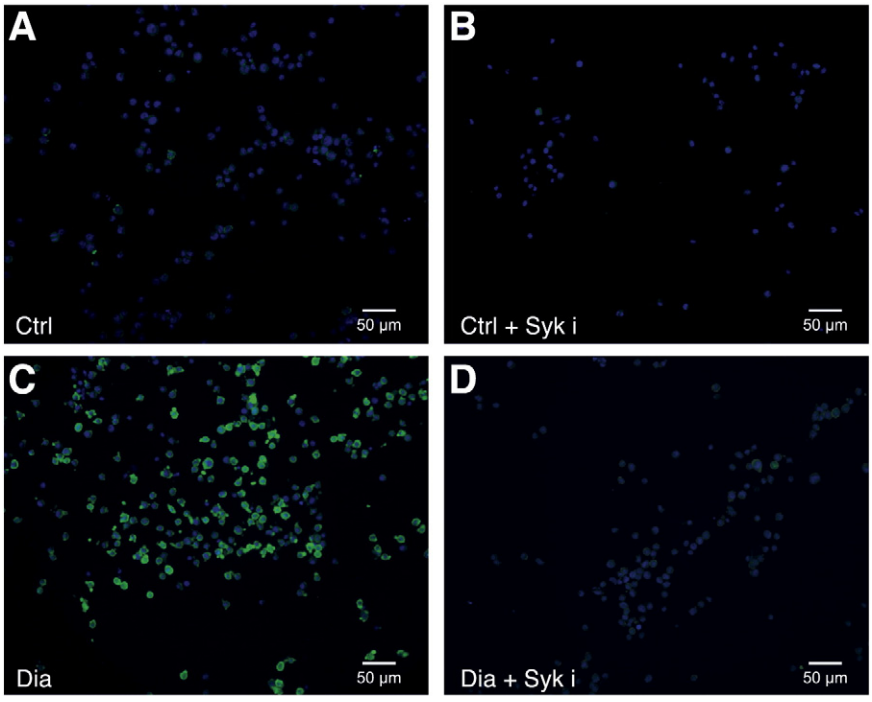

Fig. 4. Interference and phase contrast microscopy of Jurkat T cells exposed to diamide and Syk inhibitors. (A): Jurkat T cells (Control). (B): Jurkat T cells incubated with 5 μM Syk inhibitors. (C): Jurkat T cells treated with 0.3 mM diamide. (Panel D): Jurkat T cells treated with 0.3 mM diamide and pre-incubated with 5 μM Syk inhibitors. All the conditions were stained with FITC-conjugated anti-phosphotyrosine and DAPI.

constitutively expressed in Jurkat T cells and that its expression is not apparently affected by diamide treatment.

On the other hand, Syk appears to be strongly phosphorylated in the presence of diamide (Fig. 3B). Syk inhibition determines a profound effect on the Tyr phosphorylation response (Fig. 3C, D). Additionally, experiments were performed with inhibitors of Lyn, which should be located upstream of Syk, and showed a strong decrease of Tyr phosphorylation (data not shown). Fluorescence microscopy of Jurkat T cells stained with anti-phosphotyrosine antibodies was also used to show the Tyr phosphorylation response induced by –SH group oxidation. Fig. 4 shows a homogeneous response of Jurkat T cells to diamide confirming the transient behavior observed with western blot analysis (Fig. 1A) and the marked effect of Syk inhibition (Fig. 4C, D and Fig. 10 in the Supplementary data).

3.5. Effects of –SH group oxidation and Syk inhibition on cytokine release and receptor expression

We performed a functional characterization of Jurkat T cells measuring by FACS analysis a set of released cytokines and the surface expression of different receptors.

Diamide exposure or Syk inhibition did not induce measurable changes in TNF release. Syk inhibitors induced a detectable decrease of TNF release only in basal samples (Fig. 5A). On the contrary, diamide stimulated the release of both interferon γ (IFNγ) and interleukin 2 (IL2) while Syk inhibition reduced the effects of diamide, in particular after 60 min incubation (Fig. 5B and C).

Different cell surface receptors showed variable responses to oxidation: the surface expression of CD62L, HLA-DR, CD45RA + was reduced following diamide treatment (Figs. 6 and 7). Syk inhibition caused a further decrease of this effect on CD62L and HLA-DR receptor (Figs. 6B_1 and 7A_1) expression, while it had not a measurable effect on CD45RA + (Fig. 7B_1). On the contrary, diamide treatment caused an increase of expression of CD25 receptor (Fig. 6A_1) and Syk inhibition reverted this phenomenon. The responses displayed different temporal patterns and were differently significant (Figs. 6A_1, B_1, 7A_1, B_1). In some instances, such as CD62L and HLA-DR, Syk inhibition caused a significant variation of the basal levels of surface receptors.

4. Discussion

T lymphocytes appear to respond to redox stress in inflammation and other pathological conditions [31]. Besides the involvement of redox-sensitive NF-kB and Nrf2 transcription factors in T cell activation [68,69] and additional evidence indicating the involvement of ROS in T cell activation and proliferation [70–72], very limited information is currently available on the regulatory and signaling mechanisms involved in ROS response. To generate specific responses, ROS need to interact with molecular sensors, likely to be cysteine residues located in regulatory elements. Through the formation of a reversible disulfide bond, sensors activates intracellular signaling pathways upon detection of redox changes [2,6,8]. To explore this mechanism, Jurkat T cells were treated with non-cytotoxic concentrations of diamide, a specific oxidant of thiol groups inducing the formation of reversible disulfide bonds. Protein Tyr phosphorylation changes were then monitored in parallel to the oxidation of protein sulfhydryl groups.

Protein Tyr phosphatase (PTPs) inhibition and Tyr kinase activation are the two mechanisms expected to regulate protein phosphorylation changes. The regulatory cysteine residues of some PTPs display a relatively low reactivity (1000-fold lower than GSH) to oxidants [52]. Keeping in consideration the high intracellular concentration of GHS, PTPs should therefore be inactivated only at very high concentrations of ROS [8].

Both Lyn and Syk tyrosine kinases appear to respond to redox changes: Lyn has been demonstrated to be a redox sensor in neutrophils [51] and Syk has been demonstrated to be reversibly activated by –SH reagents in erythrocytes [26] and B cells [73]. In the present report we have observed that, following a low-dose diamide treatment, a transient sulfhydryl group oxidation was paralleled by intense protein Tyr phosphorylation changes. Both protein Tyr phosphorylation and sulfhydryl group oxidation showed a reversible response peaking at 30 min. Interestingly, Lyn and Syk kinase inhibitors efficiently reverted those changes. The effect of both inhibitors can be explained considering that Syk can be up-regulated by Lyn in different cell models [74,75]. The finding that Syk was Tyr-phosphorylated following diamide treatment substantiated its involvement in oxidant response [26].

These results may be of particular interest for the understanding of Syk inhibitors mechanism of action in the treatment of rheumatoid arthritis, which has been often associated with ROS generation [76,77]. To gain insight into the cellular mechanisms involved in the redox response of T cells, we conducted a comprehensive investigation of the Tyr phosphorylation changes using proteomic approaches. This study provided preliminary information on several potential players such as

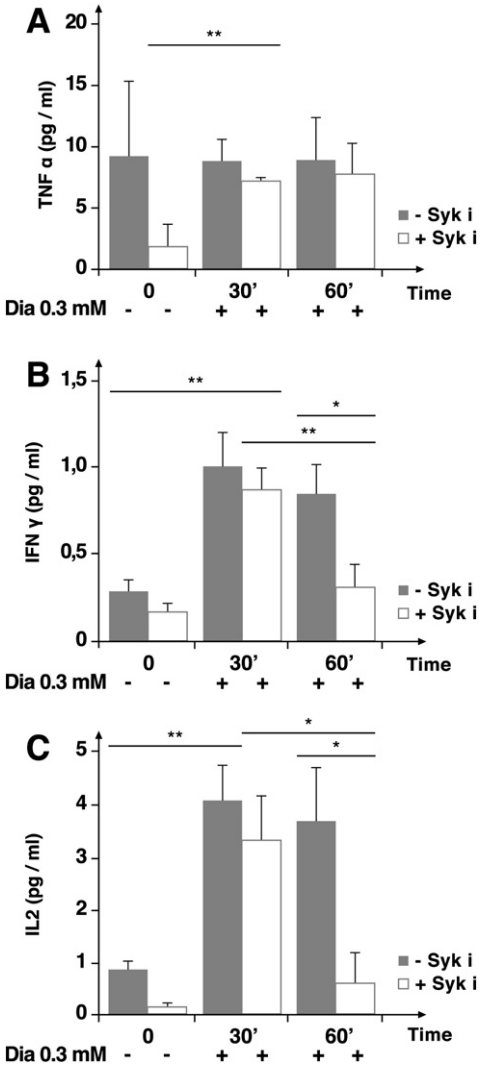

Fig. 5. Quantification analysis of TNFα, IFNγ and IL-2 cytokines released by Jurkat T cells. Jurkat T cells were treated with 0.3 mM diamide in the presence or absence of 5 μM M Syk inhibitors (Syk i). Each condition supernatant was collected, in order to evaluate the release of cytokines at different incubation times. Values are the means of 3 experiments. All data are expressed by ratio W/V in picograms (pg/ml). Medians and P values which were found to be statistically significant by the t-student test are shown (*$p < 0.05$, **$p < 0.01$, ***$p < 0.001$). (A): Jurkat T cell supernatants were probed against TNFα by CBA Flex Set method (BD Falcon). (B): Jurkat T cell supernatants were probed against IFNγ by the CBA Flex Set method (BD Falcon). (C) Jurkat T cell supernatants were probed against IL-2 by the CBA Flex Set method (BD Falcon).

AP endonucleases, Lck and Cdk3. However, proteomic data did not allow a prediction on the functional effects of protein phosphorylation changes that follow a transient sulfhydryl group oxidation.

To obtain functional data, we also monitored the variations of cytokine release and expression of a set of surface receptors following diamide treatment. In Jurkat T cells, TNF release was not affected by

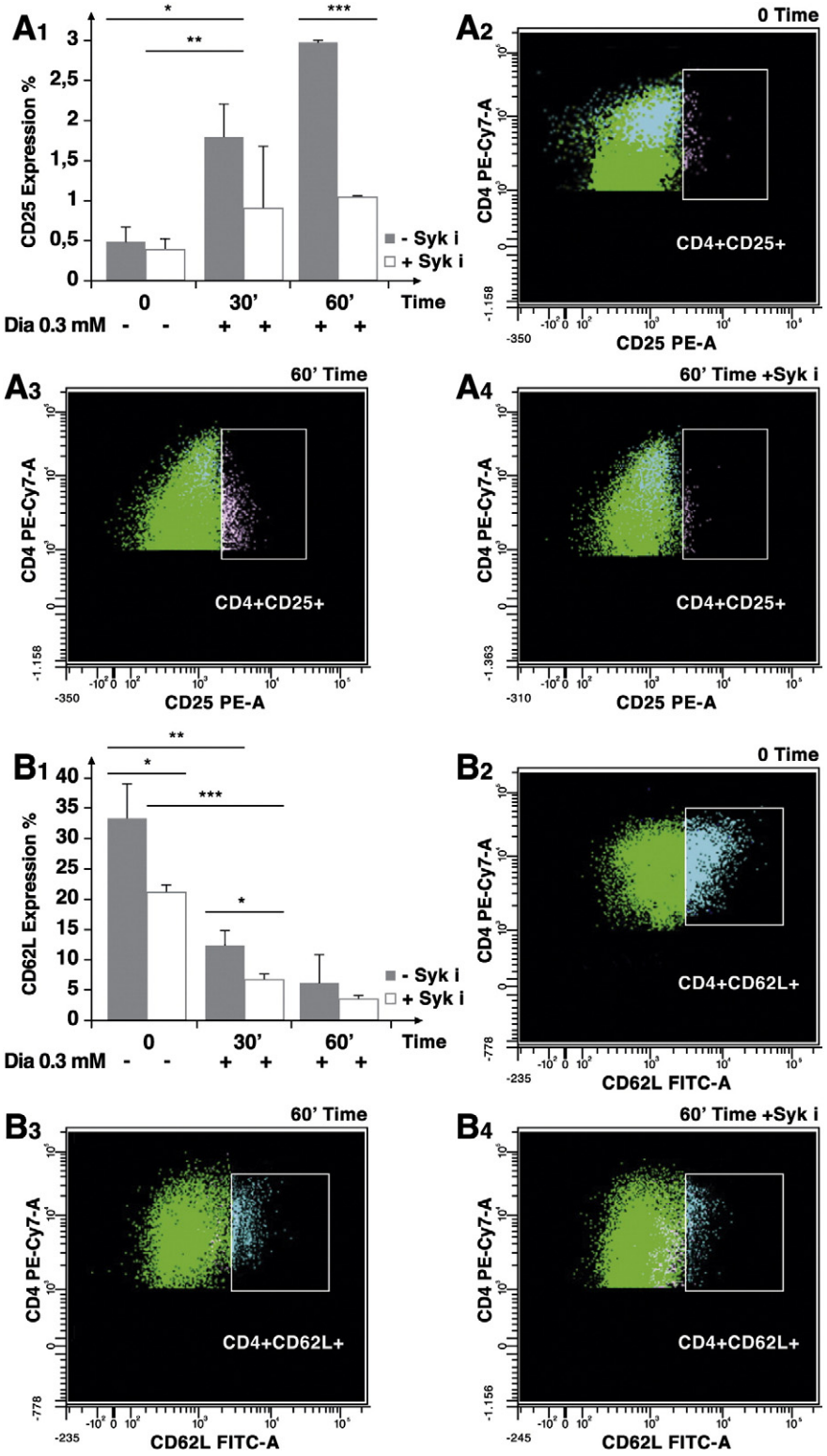

Fig. 6. CD25 and CD62L surface receptor expression of Jurkat T cells exposed to diamide and Syk inhibitors. Jurkat T cells were treated with 0.3 mM diamide in the presence or absence of 5 μM Syk inhibitors (Syk i) at different incubation times. Values are plotted as mean ± standard deviation of 3 separate experiments. All data are expressed as percent of total cell population (%). Medians and P values which were found to be statistically significant by the t-student test are shown (* $p < 0.05$, ** $p < 0.01$, *** $p < 0.001$). ($7A_1$ and $7B_1$): Jurkat T cell samples were stained against surface-CD25 and surface-CD62L analyzed by FACS. ($7A_2$, $7B_2$): Representative flow cytometric density plot of untreated Jurkat T cells stained with FITC-conjugated anti-human CD25 and CD62L. ($7A_3$, $7B_3$): Representative flow cytometric density plot of Jurkat T cells treated with 0.3 mM diamide for 1 h stained with FITC-conjugated anti-human CD25 and CD62L. ($7A_4$, $7B_4$): Representative flow cytometric density plot of Jurkat T cells treated with 0.3 mM diamide and Syk inhibitor for 1 h stained with FITC-conjugated anti-human CD25 and CD62L.

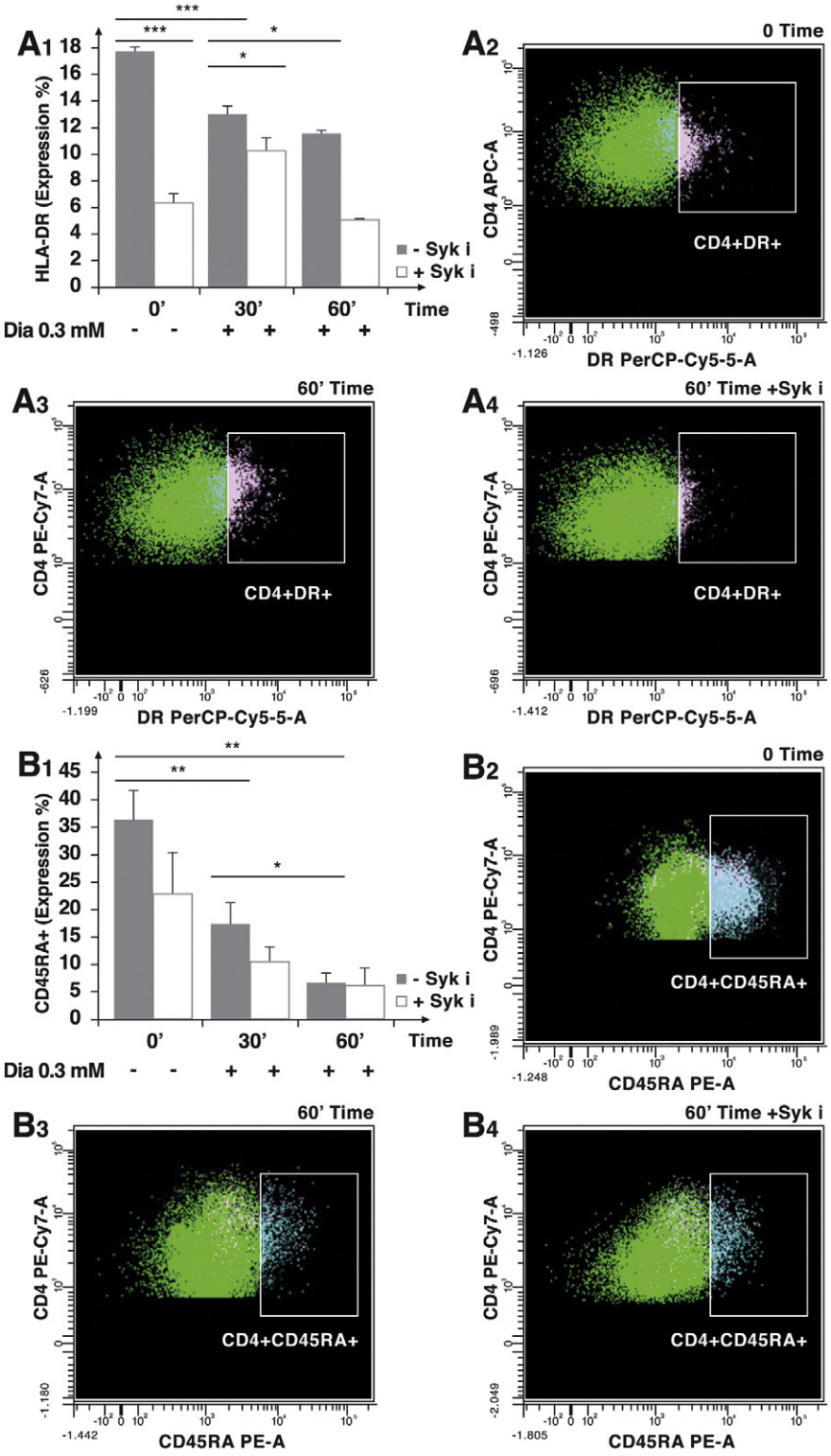

Fig. 7. HLA-DR and CD45RA+ surface receptor expression of Jurkat T cells exposed to diamide and Syk inhibitors. Jurkat T cells were treated with 0.3 mM diamide in the presence or absence of 5 μM Syk inhibitors (Syk i.) at different incubation times. Values are plotted as mean ± standard deviation of 3 separate experiments. All data are expressed as percent of total cell population (%). Medians and P values which were found to be statistically significant by the t-student test are shown (*$p < 0.05$, **$p < 0.01$, ***$p < 0.001$). ($8A_1$, $8B_1$): Jurkat T cell samples were stained against surface-HLA-DR and surface-CD45RA+ analyzed by FACS. ($8A_2$, $8B_2$): Representative flow cytometric density plot of untreated Jurkat T cells stained with FITC-conjugated anti-human HLA-DR and CD45RA+. ($8A_3$, $8B_3$): Representative flow cytometric density plot of Jurkat T cells treated with 0.3 mM diamide for 1 h stained with FITC -conjugated anti-human HLA-DR and CD45RA. ($8A_4$, $8B_4$): Representative flow cytometric density plot of Jurkat T cells treated with 0.3 mM diamide and Syk inhibitor for 1 h stained with FITC -conjugated anti-human HLA-DR and CD45RA.

diamide while IFNγ and IL2 peaked in correspondence of the maximal sulfhydryl oxidation and Tyr phosphorylation responses. Expression of CD25 (α-chain of the IL2 receptor), a late activation receptor, showed the same behavior. On the contrary, HLA-DR, an element of the MHC II, was transiently down-regulated by diamide. Diamide also caused a negative and transient effect on the surface expression of CD62L, a

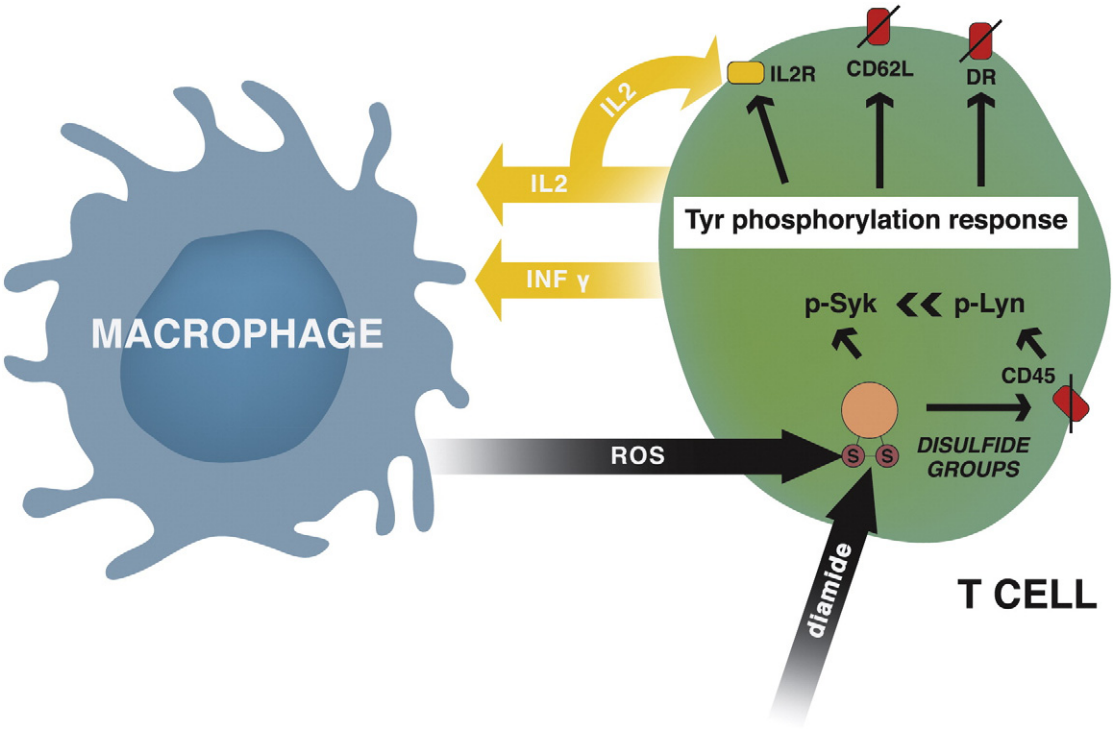

Fig. 8. Thiol group-based redox regulation model of phosphotyrosine changes in T cells. ROS from different sources, such as macrophages, may modulate tyrosine cascade in Jurkat T cells. Oxidation of cysteinil –SH groups could generate a direct activation of Syk or an inhibition of tyrosine phosphatases as CD45. CD45 block promotes phosphorylation of Lyn that activates Syk. Syk has a key role in the subsequent phosphotyrosine events. These molecular phenomena may involve a variegate number of effectors and generate a cellular response that increases the production of IL2 and the expression of its receptor (CD25) or decreases other receptors (CD62L, HLA, CD45).

selectin surface antigen expressed related to T cells homing. The Tyr phosphatase CD45RA+ also displayed a down-expression following diamide treatment. It is interesting to note that CD45 specifically dephosphorylates Lyn, consequently down-regulating its activity [78]. A down-regulation of CD45 should then induce an up-regulation of Lyn and consequently of Syk [74,79]. This finding is in agreement with the powerful effect of Lyn and Syk inhibitors on the phosphorylation response that follows diamide treatment. The efficiency of Syk inhibitors in suppressing most of the observed cellular responses to redox stress is also in agreement with a sequential involvement of Lyn and Syk.

In conclusion, in Jurkat T cells a transient oxidation of protein sulfhydryl groups induces a complex protein Tyr phosphorylation response, accompanied by intense and reversible changes of cytokines release and receptors exposure. Although the physiological meaning of the observed changes is still difficult to assess, in Fig. 8 we propose an interpretation of the T cell response to the redox stress generated during inflammation: i) the observed release of IFNγ by T cells may activate macrophages eliciting a positive feedback for ROS production; ii) the release of IL2 and the over-expression of IL2 receptor may induce T cell proliferation but also further macrophage and killer cells activation; iii) the down-regulation of CD62L receptor and the lack of effects on TNF release indicate a multifaceted response of T cells; iv) the putative effect of CD45 inhibition on Lyn and Syk activation have also been depicted.

The interpretation of our results should also take into account the response of different T cells subsets and the modulation exerted by the large number of regulatory signals that may accompany the production of ROS during inflammation.

List of Abbreviations

AP	apurinic/apyrimidinic endonuclease
AP-1	activator protein 1
BCR	B cell antigen receptor
BSA	Bovine Serum Albumin
CD16	cluster of differentiation 16
CD25	cluster of differentiation 25
CD3	cluster of differentiation 3
CD45	cluster of differentiation 45
CD45RA+	cluster of differentiation 45 RA+
CD45RO+	cluster of differentiation 45 RO+
CD62L	L-selectin
Cdk3	cyclin-dependent kinase 3
Cys	cysteine
DAPI	4′,6-Diamidino-2-Phenylindole
DIA	diamide
DMSO	dimethyl sulfoxide
ERK	extracellular-signal-regulated kinase
FA	fluoroacetic acid
FACS	fluorescence-activated cell sorting
FASP	filter-aided sample preparation
FBS	fetal bovine serum
FcγRI	fc-gamma receptor 1
FITC	fluorescein isothiocyanate
G6PD	glucose-6-phosphate dehydrogenase
GAPDH	glyceraldehyde 3-phosphate dehydrogenase
GSH	glutathione
H_2O_2	hydrogen peroxide
HLA-DR	human leukocyte Antigen DR
HSPs	heat shock proteins
IFNγ	interferon γ
IL2	interleukin 2
IL-2R	interleukin 2 Receptor
JAK	janus kinase
STAT	signal transducer and activator of transcription
JNK/ERK	c-jun N-terminal kinase/extracellular-signal-regulated kinase
JUNK	c-jun N-terminal kinases

LcK lymphocyte-specific protein tyrosine kinase
LPS lipopolysaccharide
Lyn lyrosine-protein kinase
MALDI matrix-assisted laser desorption/ionization
MHC II major histocompatibility complex II
MS/MS spectrometry mass/mass Spectrometry
MTT thiazolyl blue tetrazolium bromide
NF-KB nuclear factor kappa-light-chain-enhancer of activated B cells
Nrf2 NF-E2-related factor 2
p38-MAPK p38-mitogen-activated protein kinase
PBLs peripheral blood leucocytes
PBS phosphate buffer saline
PFA paraformaldehyde
PI3K/AKT phosphoinositide 3-kinase/protein kinase B
PMF peptide pass fingerprint
PP2 selective inhibitor of the Src family of protein tyrosine kinases
PRX peroxiredoxin
PTPs protein tyrosine phosphatases
RA rheumatoid arthritis
RBCs red blood cells
ROS Reactive Oxygen Species
SDS sodium dodecyl sulfate
SDS-PAGE sodium dodecyl sulfate polyacrylamide gel electrophoresis
SFK Src family kinase
SH2 domain src homology 2 domain
SHP-2 SH2 domain protein tyrosine phosphatase-2
SLE systemic lupus erythematosus
Syk spleen tyrosine kinase
SykI Syk inhibitors II
TAM tumor-associated macrophages
TCR t cell receptor
TFA trifluoroacetic acid
TNF tumor necrosis factor
ToF time of flight
Treg regulatory t cells
TRX thioredoxine
Tyr tyrosine

Supplementary data to this article can be found online at http://dx.doi.org/10.1016/j.cellsig.2014.12.014.

Acknowledgments

We are thankful for the scientific and technical support of Prof. Elizabeth Komives in the Department of Chemistry and Biochemistry at UCSD (California), Dr. Marianna Greco in the Department of Medical Sciences, (University of Cagliari, Italy), Prof. Luigi Sciola, Prof. Roberto Manetti and Giuseppe Delogu in the Department of Biomedical Sciences (University of Sassari, Italy). This work was supported by funds of the Bank of Sardinia Foundation (Fondazione Banco di Sardegna), grant number U712.2013/AI.636.MGB.

References

[1] M.L. Circu, T.Y. Aw, Free Radic. Biol. Med. 48 (2010) 749–762.
[2] C. Klomsiri, P.A. Karplus, L.B. Poole, Antioxid. Redox Signal. 14 (2011) 1065–1077.
[3] P.D. Ray, B.W. Huang, Y. Tsuji, Cell. Signal. 24 (2012) 981–990.
[4] M. Schieber, N.S. Chandel, Curr. Biol. 24 (2014) R453–R462.
[5] S. Biswas, A.S. Chida, I. Rahman, Biochem. Pharmacol. 71 (2006) 551–564.
[6] L.B. Poole, K.J. Nelson, Curr. Opin. Chem. Biol. 12 (2008) 18–24.
[7] S.E. Ryu, J. Biochem. 151 (2012) 579–588.
[8] C.C. Winterbourn, M.B. Hampton, Free Radic. Biol. Med. 45 (2008) 549–561.
[9] N. Brandes, S. Schmitt, U. Jakob, Antioxid. Redox Signal. 11 (2009) 997–1014.
[10] K.S. Doris, E.L. Rumsby, B.A. Morgan, Mol. Cell. Biol. 32 (2012) 4472–4481.
[11] H. Miki, Y. Funato, J. Biochem. 151 (2012) 255–261.
[12] S.G. Rhee, H.Z. Chae, K. Kim, Free Radic. Biol. Med. 38 (2005) 1543–1552.
[13] C.Y. Chen, D. Willard, J. Rudolph, Biochemistry 48 (2009) 1399–1409.
[14] M.J. Morgan, Z.G. Liu, Cell Res. 21 (2011) 103–115.
[15] F.J. Staal, M. Roederer, L.A. Herzenberg, L.A. Herzenberg, Proc. Natl. Acad. Sci. U. S. A. 87 (1990) 9943–9947.
[16] M. Karin, E. Shaulian, IUBMB Life 52 (2001) 17–24.
[17] E. Shaulian, M. Karin, Oncogene 20 (2001) 2390–2400.
[18] Y. Devary, R.A. Gottlieb, L.F. Lau, M. Karin, Mol. Cell. Biol. 11 (1991) 2804–2811.
[19] P. Klatt, E.P. Molina, M.G. De Lacoba, C.A. Padilla, E. Martinez-Galesteo, J.A. Barcena, S. Lamas, FASEB J. 13 (1999) 1481–1490.
[20] Y. Gao, A. Howard, K. Ban, J. Chandra, J. Biol. Chem. 284 (2009) 7114–7125.
[21] W.H. Kim, J.W. Lee, B. Gao, M.H. Jung, Cell. Signal. 17 (2005) 1516–1532.
[22] A. Matsuzawa, H. Ichijo, Biochim. Biophys. Acta 1780 (2008) 1325–1336.
[23] A. Rivera, S.A. Maxwell, J. Biol. Chem. 280 (2005) 29346–29354.
[24] H.M. Shen, Z.G. Liu, Free Radic. Biol. Med. 40 (2006) 928–939.
[25] P. Heneberg, L. Dráberová, M. Bambousková, P. Pompach, P. Dráber, J. Biol. Chem. 285 (2010) 12787–12802.
[26] A. Pantaleo, E. Ferru, G. Giribaldi, F. Mannu, F. Carta, A. Matte, L. de Franceschi, F. Turrini, Biochem. J. 418 (2009) 359–367.
[27] E. Ferru, K. Giger, A. Pantaleo, E. Campanella, J. Grey, K. Ritchie, R. Vono, F. Turrini, P.S. Low, Blood 117 (2011) 5998–6006.
[28] A. Siciliano, F. Turrini, M. Bertoldi, A. Matte, A. Pantaleo, O. Olivieri, L. De Franceschi, Blood Cells Mol. Dis. 44 (2010) 233–242.
[29] F. Turrini, G. Giribaldi, F. Carta, F. Mannu, P. Arese, Redox Rep. 8 (2003) 300–303.
[30] J.M. Gostner, K. Becker, D. Fuchs, R. Sucher, Redox Rep. 18 (2013) 88–94.
[31] P. Kesarwani, A.K. Murali, A.A. Al-Khami, S. Mehrotra, Antioxid. Redox Signal. 18 (2013) 1497–1534.
[32] Y. Zhao, B. Zhao, Oxid. Med. Cell. Longev. 2013 (2013) 316523. http://dx.doi.org/10.1155/2013/316523.
[33] C. Wersinger, A. Sidhu, Curr. Med. Chem. 13 (2006) 591–602.
[34] M. Iborra, I. Moret, F. Rausell, G. Bastida, M. Aguas, M. Cerrillo, P. Nos, B. Beltran, Biochem. Soc. Trans. 39 (2011) 1102–1106.
[35] D. Shah, N. Mahajan, S. Sah, S.K. Nath, B. Paudyal, J. Biomed. Sci. 21 (2014) 23. http://dx.doi.org/10.1186/1423-0127-21-23.
[36] S. Kundu, P. Ghosh, S. Datta, A. Ghosh, S. Chattopadhyay, M. Chatterjee, Free Radic. Res. 46 (2012) 1482–1489.
[37] B. Wilkinson, J.S. Downey, C.E. Rudd, Expert Rev. Mol. Med. 7 (2005) 1–29.
[38] K.R. Olson, N.L. Whitfield, Antioxid. Redox Signal. 12 (2010) 1219–1234.
[39] D.B. Sawyer, Am. J. Med. Sci. 342 (2011) 120–124.
[40] K. Kono, F. Salazar-Onfray, M. Petersson, J. Hansson, G. Masucci, K. Wasserman, T. Nakazawa, P. Anderson, R. Kiessling, Eur. J. Immunol. 26 (1996) 1308–1313.
[41] R. Lichtenfels, D. Mougiakakos, C.C. Johansson, S.P. Dressler, C.V. Recktenwald, R. Kiessling, B. Seliger, PLoS One 7 (2012) e41345.
[42] K.J. Malmberg, V. Arulampalam, F. Ichihara, M. Petersson, K. Seki, T. Andersson, R. Lenkei, G. Masucci, S. Pettersson, R. Kiessling, J. Immunol. 167 (2001) 2595–2601.
[43] M. Otsuji, Y. Kimura, T. Aoe, Y. Okamoto, T. Saito, Proc. Natl. Acad. Sci. U. S. A. 93 (1996) 13119–13124.
[44] T. Aoe, Y. Okamoto, T. Saito, J. Exp. Med. 181 (1995) 1881–1886.
[45] J.W. Baty, M.B. Hampton, C.C. Winterbourn, Biochem. J. 389 (2005) 785–795.
[46] D. Mougiakakos, C.C. Johansson, R. Kiessling, Blood 113 (2009) 3542–3545.
[47] P. Chiarugi, G. Pani, E. Giannoni, L. Taddei, R. Colavitti, G. Raugei, M. Symons, S. Borrello, T. Galeotti, G. Ramponi, J. Cell Biol. 161 (2003) 933–944.
[48] I.V. Klyubin, K.M. Kirpichnikova, I.A. Gamaley, Eur. J. Cell Biol. 70 (1996) 347–351.
[49] J.R. Mathias, B.J. Perrin, T.X. Liu, J. Kanki, A.T. Look, A. Huttenlocher, J. Leukoc. Biol. 80 (2006) 1281–1288.
[50] P. Niethammer, C. Grabher, A.T. Look, T.J. Mitchison, Nature 459 (2009) 996–999.
[51] S.K. Yoo, T.W. Starnes, Q. Deng, A. Huttenlocher, Nature 480 (2011) 109–112.
[52] A. Salmeen, D. Barford, Antioxid. Redox Signal. 2005 (7) (2005) 560–577.
[53] J.J. Tanner, Z.D. Parsons, A.H. Cummings, H. Zhou, K.S. Gates, Antioxid. Redox Signal. 15 (2011) 77–97.
[54] J.Y. Jang, J.H. Min, Y.H. Chae, J.Y. Baek, S.B. Wang, S.J. Park, G.T. Oh, S.H. Lee, Y.S. Ho, T.S. Chang, Antioxid. Redox Signal. 20 (2014) 2528–2540.
[55] M.B. Humphrey, L.L. Lanier, M.C. Nakamura, Immunol. Rev. 208 (2005) 50–65.
[56] S. Yanagi, T. Kurosaki, H. Yamamura, Cell. Signal. 7 (1995) 185–193.
[57] E. Arias-Palomo, M.A. Recuero-Checa, X.R. Bustelo, O. Llorca, Biochim. Biophys. Acta 1774 (2007) 1493–1499.
[58] S. Qin, T. Kurosaki, H. Yamamura, Biochemistry 37 (1998) 5481–5486.
[59] D. Mourao-Sa, M.J. Robinson, S. Zelenay, D. Sancho, P. Chakravarty, R. Larsen, M. Plantinga, N. Van Rooijen, M.P. Soares, B. Lambrecht, C. Reis e Sousa, Eur. J. Immunol. 41 (2011) 3040–3053.
[60] T. Lebouvier, T.M. Scales, D.P. Hanger, R.L. Geahlen, B. Lardeux, C.H. Reynolds, B.H. Anderton, P. Derkinderen, Biochim. Biophys. Acta 1783 (2008) 188–192.
[61] L.Y. Moy, Y. Jia, M. Caniga, G. Lieber, M. Gil, X. Fernandez, E. Sirkowski, R. Miller, J.P. Alexander, H.H. Lee, J.D. Shin, J.M. Ellis, H. Chen, A. Wilhelm, H. Yu, S. Vincent, R.W. Chapman, N. Kelly, E. Hickey, W.M. Abraham, A. Northrup, T. Miller, H. Houshyar, M.A. Crackower, Am. J. Respir. Cell Mol. Biol. 49 (2013) 1085–1092.
[62] P.J. Coopman, S.C. Mueller, Cancer Lett. 241 (2006) 159–173.
[63] G. Feng, X. Wang, Lymphoma (2014). http://dx.doi.org/10.3109/10428194.2014.891026.
[64] J. Hong, Y. Yuan, J. Wang, Y. Liao, R. Zou, C. Zhu, B. Li, Y. Liang, P. Huang, Z. Wang, W. Lin, Y. Zeng, J.L. Dai, R.T. Chung, Cancer Res. 74 (2014) 1845–1856.
[65] L. Bordin, F. Ion-Popa, A.M. Brunati, G. Clari, P.S. Low, Biochim. Biophys. Acta 1745 (2005) 20–28. http://dx.doi.org/10.1016/j.bbamcr.2004.12.010.
[66] H. Bartsch, J. Nair, Langenbecks Arch. Surg. 391 (2006) 499–510.
[67] A. Federico, F. Morgillo, C. Tuccillo, F. Ciardiello, C. Loguercio, Int. J. Cancer 121 (2007) 2381–2386.
[68] C. Morzadec, M. Macoch, L. Sparfel, S. Kerdine-Römer, O. Fardel, L. Vernhet, Free Radic. Biol. Med. 71 (2014) 133–145.
[69] K. Schulze-Osthoff, M. Los, P.A. Baeuerle, Biochem. Pharmacol. 50 (1995) 735–741.

[70] J.P. Secrist, L.A. Burns, L. Karnitz, G.A. Koretzky, R.T. Abraham, J. Biol. Chem. 268 (1993) 5886–5893.
[71] M. Suthanthiran, M.E. Anderson, V.K. Sharma, A. Meister, Proc. Natl. Acad. Sci. U. S. A. 87 (1990) 3343–3347.
[72] F.B. Thoren, A. Betten, A.I. Romero, K. Hellstrand, J. Immunol. 179 (2007) 21–25.
[73] T. Takano, K. Sada, H. Yamamura, Antioxid. Redox Signal. 4 (2002) 533–541.
[74] T. Kurosaki, S.A. Johnson, L. Pao, K. Sada, H. Yamamura, J.C. Cambier, J. Exp. Med. 179 (1994) 1725–1729.
[75] S. Muthukkumar, C. Venkataraman, T. Woods, S. Bondada, Mol. Immunol. 34 (1997) 865–875.
[76] V.C. Kyttaris, G.C. Tsokos, Clin. Immunol. 124 (2007) 235–237.
[77] J.S. Nijjar, A. Tindell, I.B. McInnes, S. Siebert, Rheumatology 52 (2013) 1556–1562.
[78] A.E. Saunders, P. Johnson, Cell. Signal. 22 (2010) 339–348.
[79] L.B. Justement, Int. Rev. Immunol. 20 (2001) 713–738.